# COMPARISON OF ASYMPTOTIC AND FULL-WAVE PREDICTIONS OF INSTALLED ANTENNA PERFORMANCE ON AIRFRAMES

M. V. T. Heckler and A. Dreher
German Aerospace Center (DLR) / Institute of Communications and Navigation
Oberpfaffenhofen, 82234 Weßling
Germany

## ABSTRACT

This paper presents results from investigations carried out by DLR regarding installed performance of antennas on airframes. For the electromagnetic analyses, different simulation methods have been used. The results have been compared with measurements using a scaled mock-up at a higher frequency. The paper presents a discussion about the results obtained with both techniques, including a discretization analysis to infer whether the predictions could be still improved if the mesh modelling of the airframe is refined.

## 1. INTRODUCTION

In a contribution presented at the German Aerospace Congress 2005, the authors discussed the possibility of testing installed antenna performance using adequate electromagnetic simulators and experimental validation using mock-ups [1]. At that time, VHF (communication) and ATC (air traffic control) antennas have been analyzed. For the former case, the computations have been performed with the method of moments (MoM), which provided accurate predictions in comparison with the experimental data. The need of large computational resources is the main drawback of this method. However, since the computation domain was not large, the computations could be performed without any problems. The multi-level fast multipole method (MLFMM) has also been used and provided results very similar to the ones with MoM, with the advantage of requiring much less RAM memory.

For the ATC antennas, the operation frequency is much higher and the use of the MoM became very difficult. Therefore, since the airframe is electrically large in this case, the first analyses were performed using physical optics (PO), which is a high frequency technique suitable for this application. Multiple reflections could not be taken into account in [1], since this would have demanded very large computational effort. The simulations were therefore done considering single specular reflections only and they provided fairly accurate results, in a short time and with low memory usage. These calculations have been done within our activities in the Installed Performance of Antennas on aeroStructures (IPAS) project[1]. One of the goals of this project is to increase the accuracy of predictions of electromagnetic installed performance. For this purpose, the MLFMM has also been applied and the computed results represent better the measured data obtained with the mock-ups.

In the next sections, the simulations done with PO and MLFMM techniques are described. With the latter, more accurate results were obtained even when parts of the model, where the surface currents excited have very low levels, are completely removed, so that an incomplete airframe is considered.

Further simulations have been carried out to infer whether the mesh was fine enough to provide accurate results, as it will be described in the following sections.

## 2. PHYSICAL OPTICS COMPUTATIONS

The computations presented in this paper were performed for an ATR 42 airframe, shown in Fig. 1. The focus of this paper is the analysis of ATC antennas operating at 1 GHz. At this frequency, this aircraft is more than 70 $\lambda_0$ large both in length and wingspan, where $\lambda_0$ represents the wavelength in free space. Since the computational domain is electrically large, the first computations have been performed using PO. The details about these computations are given in the next subsections.

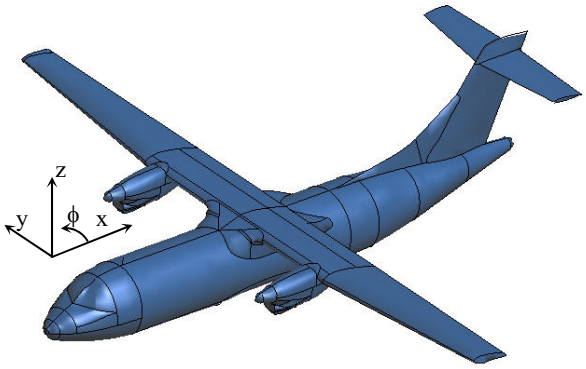


Fig. 1. CAD model of the aircraft.

### 2.1. Geometry description

One of our goals was to assess the accuracy of the electromagnetic predictions. For this purpose, the simulations have been done with the FEKO simulator [2] and the results compared with measured data. These measurements have been carried out with a 1/12$^{th}$ scaled mock-up with the antennas operating in a frequency 12 times higher than in normal operation conditions. The calculations, however, have been performed considering the airframe with full-size and at 1 GHz.

For the electromagnetic analyses, the ATC antenna was

[1] The IPAS project, Contract ref: AST3-CT2003-503611, is co-funded by the European Commission within the Sixth Framework Programme (2002 – 2007).

considered to be a monopole bent 20° (to the vertical) rearwards, with 60 mm length and 12 mm diameter. It had to be discretized in segments, as described in Fig. 2. The airframe has been modelled by a mesh composed of triangular elements that has been generated using *GiD v7.4.7b* package [3]. The monopole was fed by placing a voltage gap source on the segment connecting it to the airframe.
Since the currents on most of the surface of the airframe are not expected to vary rapidly, the triangular mesh was generated considering an edge size of $\lambda_0/5$ for the elements. On the other hand, the currents in the vicinity of the monopole vary strongly. Therefore, the mesh has been refined to $\lambda_0/10$ in this region. With this procedure, the model of the whole airframe resulted in 193212 triangles.

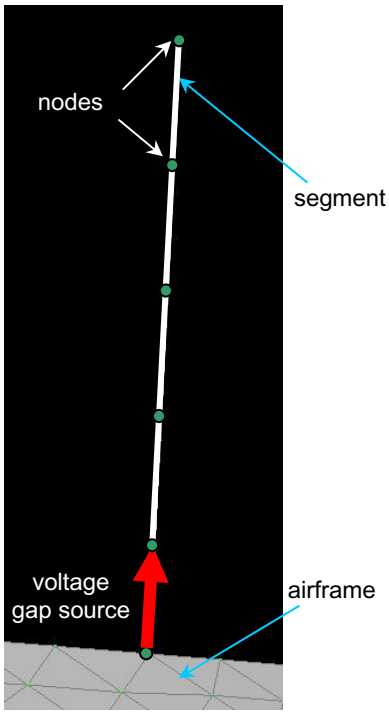


Fig. 2. Modelling of a monopole on ATR42.

The EM analyses have been performed applying a MoM/PO hybridisation, where the currents on the monopole have been computed with MoM, whereas PO has been used on the airframe. In both regions, it is assumed that segments and triangles are perfect electric conductors (PEC).

## 2.2. Results

With the model described above, simulations have been run to compute the radiation characteristics of the ATC antenna installed on the aircraft, as indicated in Fig. 3. The monopole itself cannot be seen clearly in the figure, since its length is much smaller that the dimensions of the aircraft.
Comparisons of computed with measured results in both pitch and roll planes are shown in Fig. 4 and Fig. 5. It can be seen that the predictions show an overall fair description (shape) of the radiated fields in comparison with the measurements. The levels, however, do not match very well.

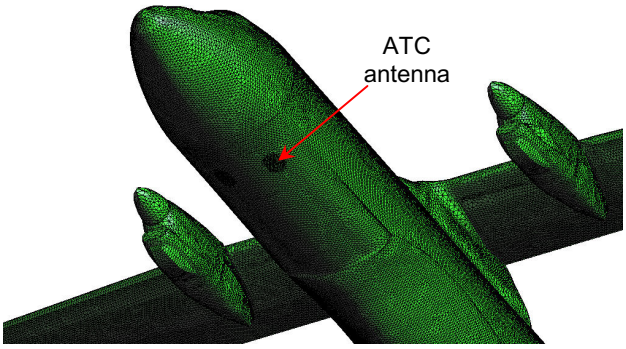


Fig. 3. Meshed model for MoM/PO analysis.

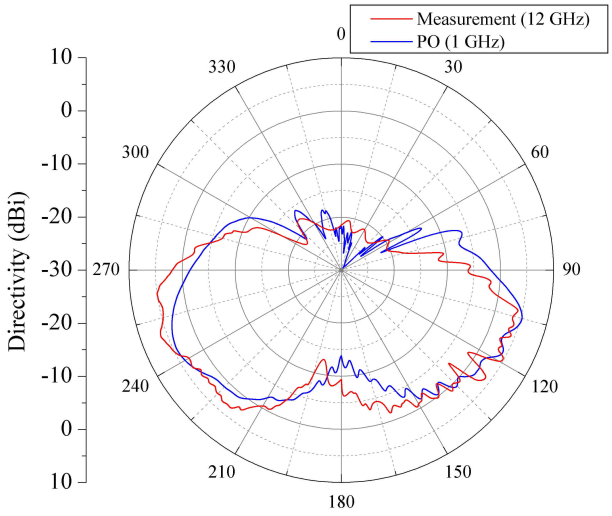


Fig. 4. Measured and computed results for the ATC antenna in the pitch plane.

The computed levels are higher in the upper forward sector, indicating that the higher (greater than one) order multiple reflections that occur in the measurements are out of phase with the direct waves and/or first order reflections, resulting in destructive interference. Since PO does not accommodate second and higher order reflections the effect of these interactions can not be seen in the computed patterns.
In the lower forward and back sectors the reverse occurs, i.e. the higher order multiple reflections that occur in the measurements are in phase with the direct waves or first order reflections causing enhancement.
As already mentioned in [1], the large mesh needed to model the airframe allowed us to consider only single specular reflections, which is a good approximation if the antenna is not installed in a critical location, where multiple reflections may play an important role [4]. As a consequence of this assumption, the curves obtained from simulated results present a relatively smooth behaviour in comparison with the experimental data.

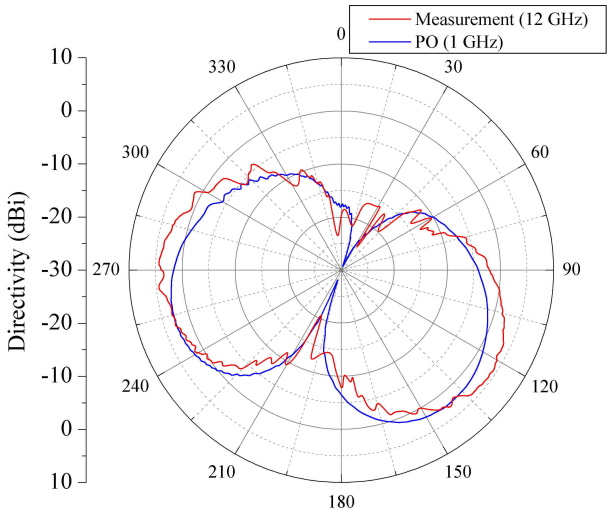


Fig. 5. Measured and computed results for the ATC antenna in the roll plane.

PO computations including the effects of multiple reflections can also be performed in FEKO by means of a visibility table [2]. This becomes too computationally expensive for large problems. Therefore, in order to improve the accuracy of the simulations, we decided to use a more precise technique, the multi-level fast multipole method, as it will be described next.

## 3. FULL-WAVE COMPUTATIONS WITH MLFMM

In order to try to improve the accuracy of the radiation pattern predictions, the same model has been simulated applying the MLFMM method. Since the airframe is a closed body, one option to improve the convergence of the preconditioner calculation would be the use of the combined-field integral equation (CFIE) approach. However, since there are open regions (monopoles) in this model, it was not possible to apply the CFIE to this structure, because the version of FEKO used at the time this computations were performed did not allow the combination of open and closed regions for MLFMM calculations. Therefore, the electric-field integral equation (EFIE) approach has been applied.

The radiation pattern predictions with the MLFMM are shown in Fig. 6 and Fig. 7. Even though the discretization over the whole aircraft is not very fine, the results agree much better with the measured curves, especially in the roll plane. One reason for that can be seen comparing the results from Fig. 8 and Fig. 9, where the current densities excited on the airframe are shown. The reason for the higher values of directivity in the roll-plane for the MLFMM results is due to the higher values of current density flowing along the circumference of the airframe. Also, since in this method all multiple reflections are taken into account, the computed radiation patterns present not a smooth profile as in the predictions with MoM/PO.

From Fig. 9, the intensity of the current densities is very low in some parts of the airplane such as on the tail fin and on the wing that is not in direct line-of-sight of the monopole. Therefore, the surface current densities excited on these parts do not contribute appreciably to the final radiation pattern. In such regions, a much coarser mesh may be generated without significant accuracy degradation.

### 3.1. Simulations of an incomplete airframe

In order to test for the influence of these currents, the tail fin, the stabilizer, the whole of starboard wing (including the engine) that is hidden from line of sight of the monopole by the fuselage as well as the upper surface of the port wing have been removed from the CAD model, as shown in Fig. 10. With the same procedure as described before, a mesh of 113530 triangles has been generated. The radiation patterns in the two principal planes are shown in Fig. 11 and Fig. 12, where it is shown that these changes in the airframe do not play a very important role. However, memory needs and computation time have been reduced.

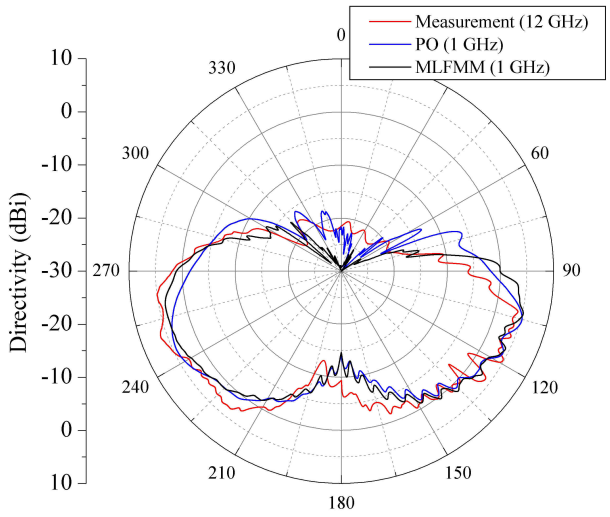


Fig. 6. Measured and computed results (with PO and MLFMM) in the pitch plane for one ATC antenna.

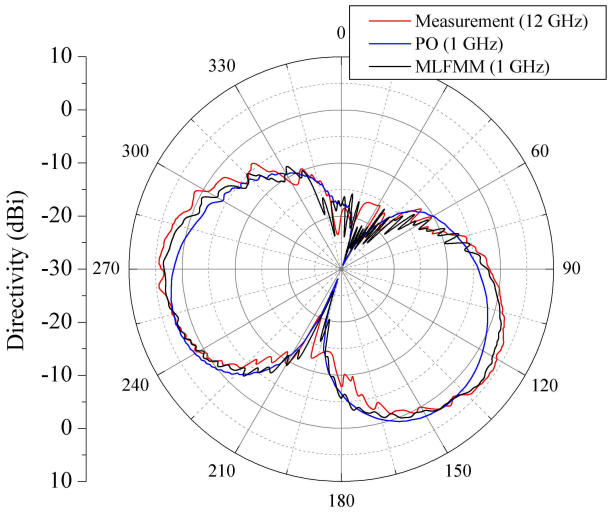


Fig. 7. Measured and computed results (with PO and MLFMM) in the roll plane for one ATC antenna.

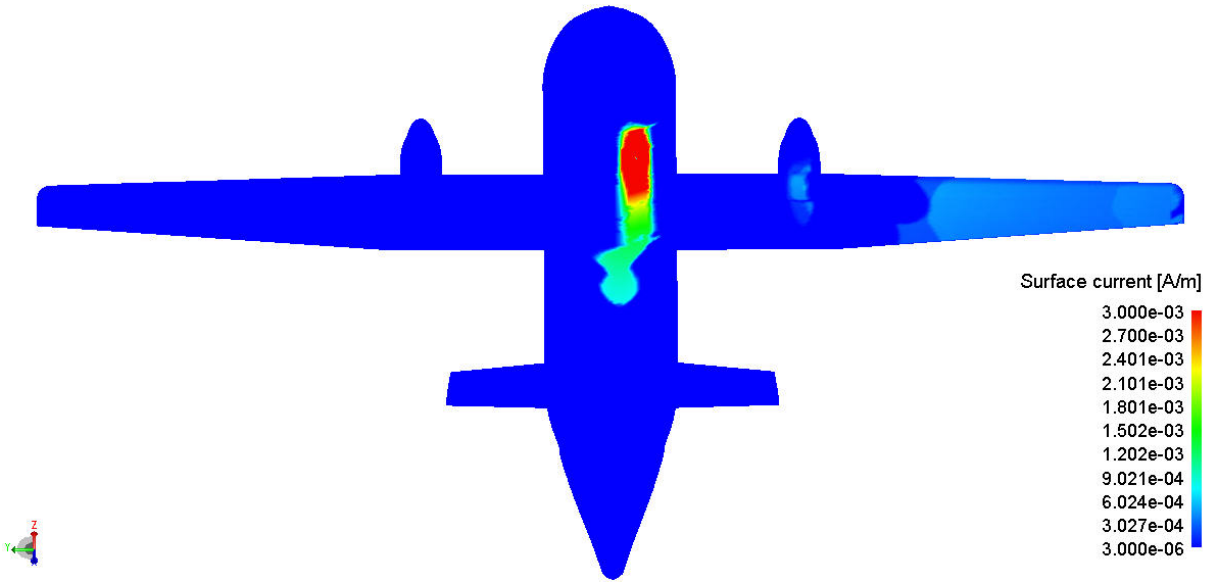


Fig. 8. Current densities on the airframe resulting from PO computations.

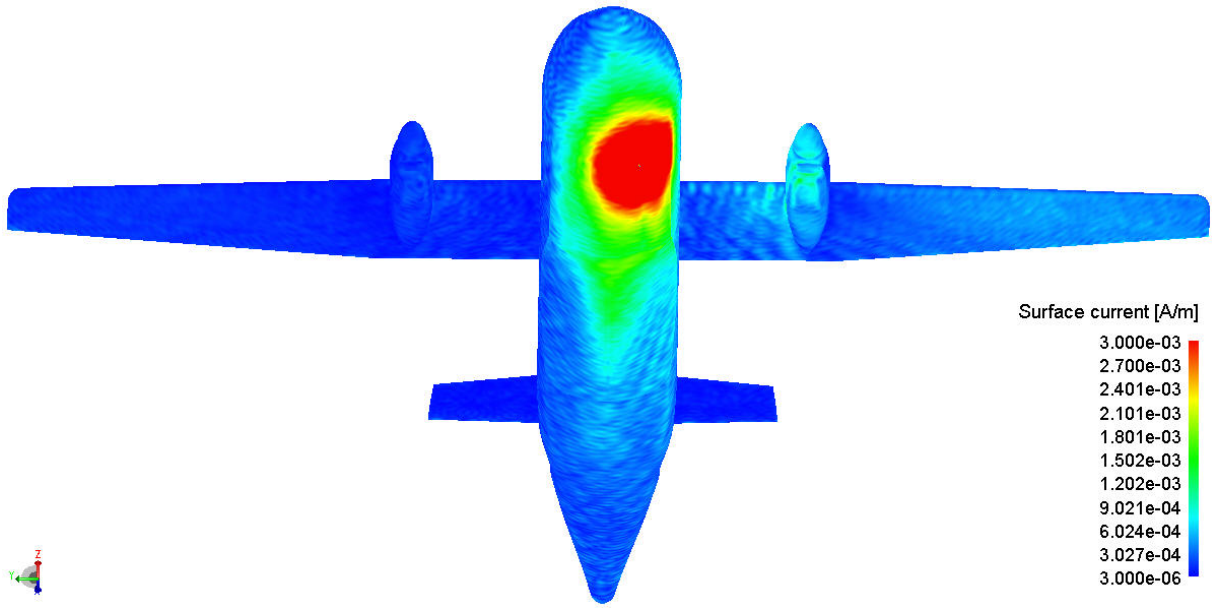


Fig. 9. Current densities on the airframe resulting from MLFMM computations.

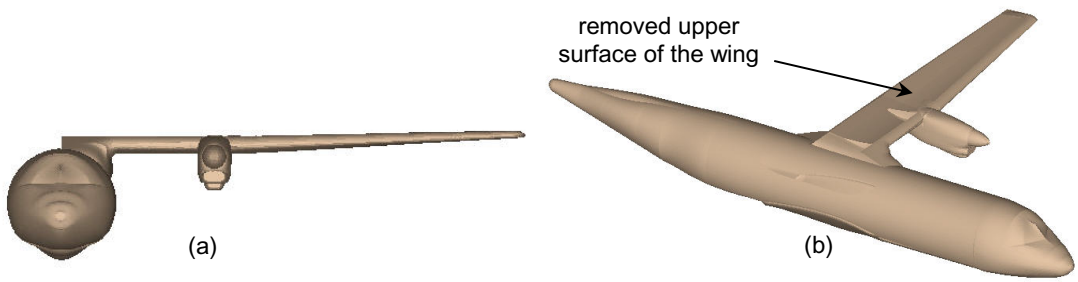


Fig. 10. CAD model showing the removed parts. (a) front view and (b) panoramic view.

| Technique | Mesh Size (triangles) | Peak Memory (GB) | Computation Time |
|---|---|---|---|
| PO/MoM | 193212 | 0.14 | 1 minute |
| MLFMM ($\lambda_0$/5) | 193212 | 2.70 | 16 hours |
| MLFMM (removed parts) | 113530 | 1.72 | 6 hours |
| MLFMM ($\lambda_0$/7) | 384180 | 6.16 | 17 hours |

Table 1. Peak memory usage and computation times for the four cases analyzed.

### 3.2. Discretization analysis

A more refined mesh for ATR42 has been generated to test whether the predictions could be still improved. Considering then an edge size of $\lambda_0$/7, the resulting mesh had 384180 triangles. For this model, similar refinement has been done in the regions surrounding the monopole ($\lambda_0$/14). The comparison is finally presented in Fig. 13 and Fig. 14. As can be seen, there are no significant differences between the two computational results, although for the latter case ($\lambda_0$/7) the size of the mesh is almost two times larger than the former.

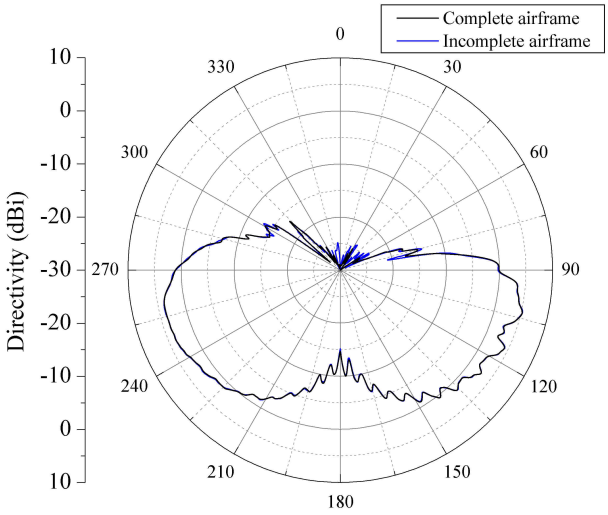


Fig. 11. Radiation pattern predictions in the pitch plane before and after removing parts of the airframe applying the MLFMM for an ATC antenna.

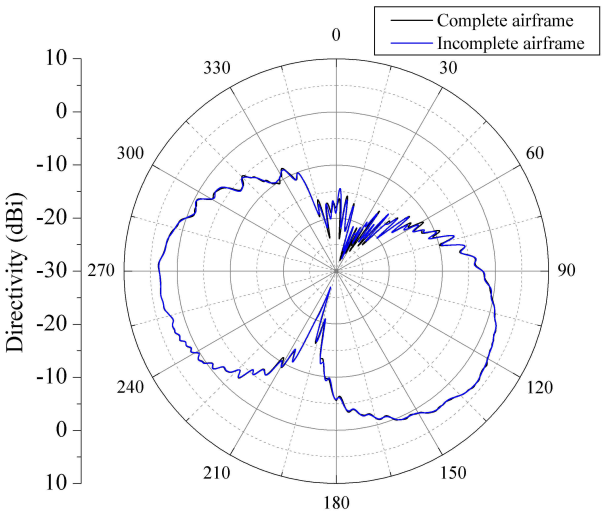


Fig. 12. Radiation pattern predictions in the roll plane before and after removing parts of the airframe applying the MLFMM for an ATC antenna.

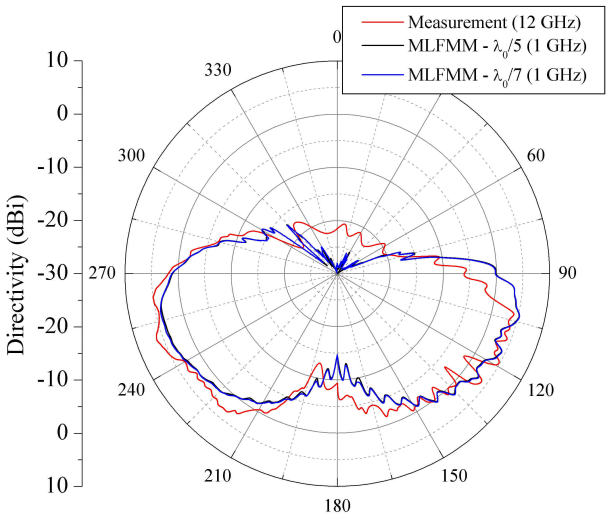


Fig. 13. Comparison of radiation pattern simulated and measured in the pitch plane for different discretization criteria applying the MLFMM for an ATC antenna.

## 4. COMPUTATION TIME AND MEMORY USAGE

Apart from the accuracy of the results, other important characteristics of numerical methods are the time and RAM memory needed for the simulations. Table 1 gives these details for all the four cases considered in this paper. The computer was an AMD Opteron™ Processor 250, 2.39 GHz.

## 5. CONCLUSION

At 1 GHz, the electrical dimensions of ATR 42 are already large for the application of the conventional MoM. Therefore, the first predictions were performed using a hybridisation of PO/MoM. For the PO region, only single reflections have been considered. Further modelling has been done applying MLFMM, which resulted in an increased accuracy when comparing to the measured results, even when parts of the airframe that do not present a direct line-of-sight have been removed from the simulation. This extreme case has been analyzed to infer the influence of very low levels of surface current densities in some regions of the aircraft. Instead of simply removing parts of the airframe, it would be recommended to generate a very coarse mesh where the currents are expected to be of low intensity, if the software in use allows such flexibility. This may save memory and time for the calculations, without reducing the accuracy in the predictions.
The influence of multiple reflections on the far-field can be taken into account with the PO+MoM approach, if a visibility table is generated. However, the computational effort demanded may be even larger than for the MLFMM simulations, which provided better results and should be the preferred technique, if its application is allowed from the point of view of available computational resources.

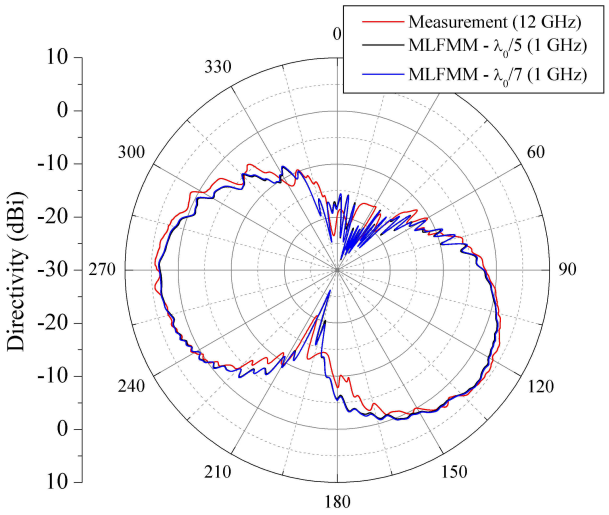


Fig. 14. Comparison of radiation pattern simulated and measured in the roll plane for different discretization criteria applying the MLFMM for an ATC antenna.

## 6. ACKNOLEDGEMENTS

The authors would like to thank to ATR (Avions de Transport Regional) for providing the original CAD model and the experimental data, and to EADS-CCR (EADS Common Research Center in France) and ONERA (Office National d'Etudes et de Recherches Aérospatiales) for providing a cleaned version of the CAD model used on the analyses presented in this paper.
The authors are grateful for the valuable comments and review of the manuscript done by Mrs. Thereza Macnamara, from BAE Systems – UK.

## 7. REFERENCES

[1] M. V. T. Heckler and A. Dreher, "Comparison of predicted and measured radiation patterns of monopoles on scaled airframes," Proceedings of the German Aerospace Congress 2005, Friedrichshafen, Germany, Sep. 2005.
[2] *FEKO© user's manual*, EM Software & Systems – S.A. (Pty) Ltd, Jul. 2005.
[3] *GiD version 7.4.4b user's manual*, International Centre for Numerical Methods in Engineering, Oct. 2003.
[4] J. Péres, J. A. Saiz, O. M. Conde, R. P. Torres, and M. F. Cátedra, "Analysis of antennas on board arbitrary structures modeled by NURBS surfaces," *IEEE Trans. Antennas Propagat.*, vol. 45, pp.1045 – 1053, Jun. 1997.